Localization, collision avoidance, and centroid navigation of parachutes swarm

Niccolò Andreetta
niccolo.andreetta@studenti.unitn.it
M.N. 232077

Simone Manfredi
simone.manfredi@studenti.unitn.it
M.N. 239337

***Abstract*—This project deals with the localization and control of a swarm of parachutes intended to be dropped from a certain height and autonomously reach a desired location on the ground. In particular, each agent controls its movement to drive the centroid of the storm towards the desired final location.**
The parachutes are firstly modelled as devices able to move independently along the three cartesian axes (thanks to an actuator in each of them), while later, they are modelled as unicycles with forward velocity, rotation and falling velocity controls.
The main features that each parachute has to implement are self-localization in the space (via absolute and relative position measurement), the optimal control to design the trajectory to be followed, and collision avoidance.
The simulation results show that the parachutes can accomplish their task and reach the ground without any collision, even in the presence of noises in the inputs, dynamics and GPS tracking.

I. Introduction

The fields of distributed systems and optimal control play an essential role in modern problems, such as precision-guided parachutes for cargo delivery [1] [2].
This project aims to drive the centroid of a storm of falling parachutes from the initial releasing point to the desired landing target on the ground. To pursue this purpose, each agent must always be able to identify the geometric centroid of the storm and move such that the new mean point position accomplishes what the motion trajectory planner defines. It must be noted that here, the focus is on the mean point of the formation so that the single parachutes can land in the neighbourhoods of the arrival location.
Along with the distribution of information and path control, collision avoidance is a critical requirement because any crash can lead to an uncontrolled fall of the agents.
The available hardware to each parachute is composed of some measurement systems allowing the localization in space, the communication between each other, and the measurement of relative distances.
The limitations of the scope of this project are the following: the dynamic of the parachutes is simplified, the actuators have not been practically identified, two parachutes in the storm can either communicate with one another or cannot communicate at all (i.e. unidirectional communication is not taken into account).

II. Adopted models

A. Simplified parachute model

The considered parachutes are made of two main parts: a sail with finite radial dimensions and height and a payload with dimension negligible compared to the first. The latter is placed below the former and carries also the communication, measurement and control systems.
The most simple dynamical parachute model is linear and considers three actuators able to move the device in space, while gravity acts as non-controllable input along the vertical direction.

$$x_{i+1} = Ax_i + Bu + G\nu \tag{1}$$

$$\begin{bmatrix} x_{i+1} \\ y_{i+1} \\ z_{i+1} \end{bmatrix} = I_3 \begin{bmatrix} x_i \\ y_i \\ z_i \end{bmatrix} + \Delta t I_3 \begin{bmatrix} v_x \\ v_y \\ v_z \end{bmatrix} + \begin{bmatrix} 1 & 0 & 0 & 0 \\ 0 & 1 & 0 & 0 \\ 0 & 0 & 1 & \Delta t \end{bmatrix} \begin{bmatrix} \nu_x \\ \nu_y \\ \nu_z \\ \bar{v_z} \end{bmatrix}$$

The uncertainties ν_x, ν_y, and ν_z model the wind disturbances and the error along the three directions ($[\nu_x\, \nu_y\, \nu_z] \sim \mathcal{N}(0_3, L)$), while $\bar{v_z}$ is the velocity at which the parachutes fall due to the gravity action.

$\bar{v_z}$ is the non-controllable input related to the gravity that pulls the parachute to the ground.
In this way, the total velocity in the z direction has been split into a non-controllable part, which is the one related to gravity, and into a controllable one. A parachute can reduce its falling velocity by breaking until a minimum one (necessary to avoid the closure of the sail) or accelerate up to the maximum one given by its geometry.
Following typical values for these physical parameters, for the simulation it has been chosen to set the maximum free-falling speed to 55 $\left[\mathrm{m\,s^{-1}}\right]$ [4], and a maximum falling one when the parachute is opened equal to 4.87 $\left[\mathrm{m\,s^{-1}}\right]$, considering a mass of 100 $[\mathrm{kg}]$, a drag coefficient of 1.5 and a parachute's area of 45 $\left[\mathrm{m^2}\right]$, $\bar{v}_{z,max} = \sqrt{\frac{2\,m\,g}{c_p\,\rho\,A}} = 4.87\left[\mathrm{m\,s^{-1}}\right]$ [5].
Regarding the minimum falling velocity, a value equal to 25% of the maximum one has been selected arbitrarily because it is hard to define without real experiments.
Even though a physical system able to provide the required displacement on the plane has not been identified, some minimal performances in movement and errors in the actuation have been considered.

B. Unicycle-like parachute model

A more sophisticated analysis can consider that a real parachute can brake the fall and steer by toggling the lines connecting the sail and the payload. At the same time, it has only a forward velocity. These considerations suggest that it can be modelled as a unicycle, with equations given by (2).

$$\begin{aligned} x_{i+1} &= x_i + V\cos\theta\Delta t + \nu_x \\ y_{i+1} &= y_i + V\sin\theta\Delta t + \nu_y \\ z_{i+1} &= z_i + \bar{v_z}\Delta t + v_z\Delta t + \nu_z \\ \theta_{i+1} &= \theta_i + \omega\Delta t + \nu_\theta \end{aligned} \tag{2}$$

Hence, the control inputs are the forward and the rotational velocity and the falling breaks, named V, ω, and v_z. Even though in a real parachute, a minimum forward velocity is necessary to ensure the lift force sustaining the fly, in this project, the forward velocity has been assumed to be bounded between 0 and a maximum value to simplify the control laws. For what concerns the boundaries of the inputs, a maximum forward velocity of 13 $\left[\mathrm{m\,s^{-1}}\right]$ has been selected [6] [7], while the maximum rotation speed is 0.52 $\left[\mathrm{rad\,s^{-1}}\right]$. As for the control in the vertical direction, the same holds from the linear model.

C. Communication system

The adopted communication system has to allow bidirectional data exchange between chutes moving in the space. For example, this can be achieved by using a UWB mounted on the payload, which has a typical communication range of 50 $[\mathrm{m}]$ [3].
The measurement of the absolute position is done using a GPS, with an uncertainty of 5 $[\mathrm{m}]$ while for what concerns the relative measurement, multiple technologies can be used such as LIDAR, stereo camera or the combination of a UWB and a camera. For the seek of the thesis, it is assumed that the relative measurement can be done when the agents are closer than 50 $[\mathrm{m}]$ and are provided with an uncertainty of 1 $[\mathrm{m}]$. It is also assumed that each agent can measure its orientation with respect to a fixed direction but cannot measure the others'.

III. Solution

A. Localization

For the localisation, a Kalman Filter (KF) or Extended Kalman Filter (EKF) [8] (according to the considered dynamic) and a distributed Weighted Least Square (WLS) have been used. In particular, each agent localises itself by running a KF/EKF that updates its prediction with only an absolute measurement (i.e. from the GPS). In the following step, each agent measures the relative distance from the others and then projects them back in the world reference frame (i.e. a frame common for all the parachutes). Finally, the network runs a distributed WLS to share the knowledge with the team in a distributed way. The KF/EKF works as an optimal filter under the hypothesis that the noise acting on the system is white, gaussian with zero mean, and uncorrelated from the one acting on the measurement, the sensors are calibrated and affected by a zero mean white noise.
To reach the average consensus, the transition matrix describing the system at each time step has to be doubly stochastic, implying that the communication between agents has to be bidirectional.
The distribution of the localisation has been done by applying the distributed WLS algorithm presented in the course [14], with the Metropolis-Hastings weighting that ensures faster convergence with respect to the Maximum Degree [14]. In particular, each agent *i* able to communicate with another shares its localisation and the one done on the others *j* in the swarm, alongside the associated covariance matrices. The assumption on which the algorithm is based is that the localisation done by *i* on the agent j_1 is uncorrelated to the one done on j_2, which implies that the covariance matrix (called C in [14]) build during the consensus is block diagonal (even though each block is not necessarily diagonal).
The result of the consensus is that each agent may have improved the localisation on others that have already seen, but also for some further that were not directly measured before, and for which the information comes with message exchange. Note that now, the self-localisation of agent *i* depends also on the self-localisation of the others (which is embedded in the relative measurement). This implies that agent *i* cannot use the consensus output as input of the new round of KF/EKF because KFs/EKFs cannot be used in cascade. For this reason, before running another round of localisation, each agent discards the information of its position reached with the WLS. Hence, the *previous* at KF/EKF step k+1 is the output of step k. This is done to ensure that the input of a KF is uncorrelated from the output of the others.
The picture considers the probability of performing the GPS and the relative distance measurement.

B. Collision avoidance

After localising each agent, collision avoidance is necessary to let each robot be reasonably further from the others to avoid getting tangled when moving in space. This requirement must also be fulfilled while the agents are moving in a 3D environment, considering the parachute's finite size and the knowledge of the position of only a subset of agents (with a certain level of uncertainty). All these features may be well obtained by dividing the working space with a Voronoi tessellation and enforcing each agent to move remaining inside its cell.
The basic idea behind the tessellation is to assign to an agent *i* all the points of the mission space $q \in \mathcal{Q} \subseteq \mathbb{R}^2$ closer to it more than to the others agents *j* [9]:

$$\mathcal{V}_i = \left\{ q \in \mathcal{Q} | \|q - p_i\| \leq \|q - \hat{p_j}\|, \forall j \neq i, j \in \tilde{\mathcal{N}_i} \right\} \tag{3}$$

where $p_i = [x_i, y_i]^T$ is the location of the agent *i* while $\hat{p_j}$ is the one of agent *j* (eventually properly projected to achieve some further features, as will be explained in section IV).
The decentralisation of the algorithm implies that each agent performs the tessellation of only a surrounding area of radius

R_s, called *sensing range*, which is usually set at $R_s = R_c/2$, with R_c the furthest distance from where an agent can measure the position of another, called *communication range*. The *neighbour set* $\tilde{\mathcal{N}}_i$ is composed of all the agents for which the position is known either by consensus or direct measure.
During the navigation, the entity used to represent the agent is its centroid. Hence, all the computations are done to ensure that this specific point remains inside the designed area. The finite dimension of the agent δ_i has to be taken into account because otherwise, the parachute may exceed the prescribed limit even though its centroid remains inside the cell. To avoid this, the dimension of the tessellation has to be shrunk such that when the centre of the agent reaches the new edge, its encumbrance arrives at the old limit. Furthermore, since the algorithm is implemented in discrete time, the system's evolution between one instant and the following has to be considered beforehand, assuming that the agent may always move of the maximum amount allowed by the actuators in one time step.
Given that the environment where the parachutes fly is a 3D space, the Voronoi tessellation must be expanded at the whole volume of movement. However, the problem can still be seen as a planar one by projecting the location of the surrounding agents in the plane of the one doing the tessellation when these are reasonably close to each other. Furthermore, if the chute admits an actuation in the vertical direction, then the tessellation concept can be extended in the vertical axis to ensure collision avoidance even in that dimension. The safe space is between the agents and a minimum height called z_{min}.

C. High-level motion control

The high-level motion control deals with the problem of how and where to move the centroid to make it land on the target. Furthermore, since the centroid is a function of the single parachute location, it coordinates the agents' movements to realise the prescribed centroid trajectory. Instead, the actuators commands enabling this displacement are synthesised by the *low-level controller*.
In this work, the centroid is modelled as a fictional fully actuated parachute with a linear dynamic in 2 dimensions, as shown in (4), while the gravity ensures the convergence in the z-direction.

$$\begin{bmatrix} x_{i+1} \\ y_{i+1} \end{bmatrix} = \begin{bmatrix} I_2 \end{bmatrix} \begin{bmatrix} x_i \\ y_i \end{bmatrix} + \Delta t \begin{bmatrix} I_2 \end{bmatrix} \begin{bmatrix} v_{x,i} \\ v_{y,i} \end{bmatrix} \tag{4}$$

An LQR algorithm [10] has been used to find the optimal input u to be fed to the fake agent. This algorithm can only be used for linear systems, and it finds the global optimum of the problem, which is calculated by means of a minimisation of a cost function, expressed as:

$$J = \sum_{k=t}^{N-1} x_k^T S x_k + u_k^T R u_k \tag{5}$$

where S and R are the state and input cost matrices, which can be modelled to improve the state or the input minimisation, and x and u are the actual state and input.
In the discrete time, finite horizon domain, the optimum input is given by:

$$u_t = K_t x_t \tag{6}$$

where K_t is the optimal gain matrix given by the algorithm.
Once the optimal control for the fictional robot is found, following the kinematics shown in the equations (4), its next desired position is calculated.
The computation of each parachute's desired position that realises the global centroid's desired movement is not trivial. The global centroid is a function of each parachute position, and the inverse kinematic (i.e. finding the parachutes' positions that realise a desired position of the centroid) is over-determined. Two solutions have been proposed to solve this problem. At the same time, a third one to be used in some *emergency* situations to avoid collision will be presented in subsection IV-E after the reasons why it is necessary.

1) Same control for all the chutes: A quick and intuitive but "forced" solution consists of feeding the same control input in the parachutes found in the LQR problem since if every parachute moves similarly, the global centroid will be moved accordingly.

2) Inverse kinematics: A more robust solution comes from comparing this problem to the well-known and solved problem of redundancy in robotics. In fact, as in overactuated manipulators, infinite joints' configurations realise a desired end effector position; here, infinite agents' locations realise the centroid one. However, a numerical approach has been developed in the past years to solve inverse kinematics by a *postural task*, which is just an arbitrarily chosen secondary task in the joint space that does not affect the motion of the end-effector but identifies one solution among the infinite ones [11] [12].
In this specific case, two possible secondary tasks may be to let each single agent converge toward the land target or the global centroid. The algorithm can prioritise principal or secondary requirements according to a weighting value that can be chosen arbitrarily.

D. Low-level motion control

Given the single parachute target point from the high-level control, the goal of the low-level control is to provide the input that ensures the move towards it while not exceeding the motion boundaries identified by the Voronoi tessellation.

1) Control of linear model: In the case of linear dynamics, one possible control law is the one proposed by [9]:

$$u = -k_p \left(p_i - C_{\mathcal{V}_i} \right) \tag{7}$$

$$C_{\mathcal{V}_i} = \frac{1}{M_{\mathcal{V}_i}} \int_{\mathcal{V}_i} \varphi(q)\, q dq \ , \ M_{\mathcal{V}_i} = \int_{\mathcal{V}_i} \varphi(q)\, dq \tag{8}$$

with, for the planar motion, $\varphi(q)$ is a bivariate pdf centred in the point identified by the high-level control. This law uses the property that each point inside the Voronoi cell can be reached by the agent with a straight motion.
Regarding the control on the vertical axis, as said before, the velocity input has to be constrained. In particular, a

proportional gain has been chosen to break when the z_{min} is near the parachute:

$$\begin{aligned} k_{pz} &= -\bar{v}_z / R_{sv} \\ u_{tmp} &= -\bar{v}_z - k_{pz}(z_i - z_{min,i}) \\ v_z &= \min(u_{tmp}, v_{z,min} - \bar{v}_z) \end{aligned} \tag{9}$$

In this way, when there are no parachutes under the agent i, $(z_i - z_{min,i}) = R_{sv}$ and so the control v_z is zero, meaning that there is no need to break. On the other hand, when $(z_i - z_{min,i}) = 0$, meaning that the parachute would not want to go down because the other agents are too near, the input is $v_{z,min} - \bar{v}_z$, such that when in the dynamics it is added the effect of gravity (1,2) the sum results in the minimum vertical velocity: the agent cannot stop in the air but has to descent with some velocity.
Since the external disturbances act directly on the positions, the effective velocities can be locally greater or smaller than the boundaries.

2) Control of the unicycle model: Since the trajectory followed by the non-linear agents may exceed the Voronoi cell limits if (9) is employed, a more complex one must be used. In this work, the control law (10) [13] allows to guarantee the convergence of the parachute towards the target in a fast and elegant way (without the use of a PID controller), and also to find the so-called *Feedback Motion Predict (FMP)*, which is the area that the parachute can occupy during the execution of the control law (10).

$$\begin{aligned} v_y &= k_v \max\left(0, \begin{bmatrix}\cos\theta & \sin\theta\end{bmatrix}(C_{\mathcal{V}_i} - p_i)\right) \\ \omega &= k_\omega \operatorname{atan2}\left(\begin{bmatrix}-\sin\theta \\ \cos\theta\end{bmatrix}^T (C_{\mathcal{V}_i} - p_i), \begin{bmatrix}\cos\theta \\ \sin\theta\end{bmatrix}^T (C_{\mathcal{V}_i} - p_i)\right) \end{aligned} \tag{10}$$

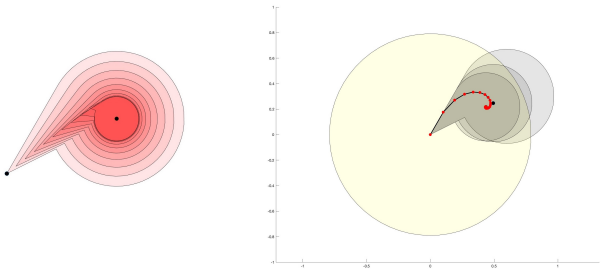

(a) *Truncated Ice-Cream Motion Cone updating as the agent moves.*

(b) *The cone is moved to be fit into the Voronoi cell.*

Fig. 1: Feedback Motion Prediction area for non-linear dynamics.

As mentioned in section II-B, the forward velocity is saturated to zero, so the parachute can never move backwards. Furthermore, it is not forced to move at a minimum velocity, as in the real chutes. This assumption simplifies the control because, in the case of non-zero positive minimum velocity (and at least with this control policy), there is no guarantee that the parachute will not exit the Voronoi cell, for example, when it is too close to the boundary.
To make sure that the parachute will not violate the Voronoi cell boundary, the FMP is initially calculated and if it exits the cell, the arrival point (i.e. the new centroid founded by (8)) is moved closer to the actual position of parachute iteratively until the FMP fits into the Voronoi cell (as could be seen in Figure 1b). [13] proposed different ways to define valid FMP, and among them, it is chosen the *Truncated Ice-Cream Motion Cone* because it is the least conservative but smaller one (Figure 1a).

IV. Implementation details

A. Structure of the simulations

The simulations can be considered as composed of four different parts.

1) Initialization: The parachutes are initially randomly located around a desired point. They have to be properly spaced since collision avoidance during the navigation is ensured only if they don't collide in the initial step, as it is expected that real parachutes are delivered reasonably far from each other.
At the beginning of the simulation, each parachute is aware of the number of agents in the swarm; it knows its position with a small uncertainty, but they do not know the location of all the other agents (so they assign a random location reasonably far from themselves with a high uncertainty to them).

2) Free falling: After the launch, the parachutes begin to accelerate downwards with closed sail and zero inputs. Only the wind disturbance can act on their position.

3) Target convergence and controlled movement: When the terminal velocity is reached, the parachutes open and begin to communicate with each other to do the Voronoi tessellation and compute the input necessary to reach the target.

4) Landing: When the agents arrive reasonably close to the ground, they start to decelerate by breaking to reach the minimum vertical velocity, arriving more gently.

B. Localization

Following the hypothesis mentioned in the subsection III-A, the measurement error, GPS tracking and wind noises/errors have been set with zero mean and Gaussian, using a random variance generator. The values of the standard deviations have already been discussed in the section II-C.
While the dynamics consider the wind effect, in the predictions step of the KF, it is supposed to be unknown; the parachute cannot measure the direction of the wind and its module. However, the variance of the wind disturbance is considered to be known, and it is included in the update of the covariance matrix of the estimated position (12). In the equation are involved the model matrices A, B and G and the covariance matrix of the wind disturbance L, while the wind effect is set to zero.

$$x_{est} = Ax_{est} + Bu + G\begin{bmatrix}0 & 0 & 0 & \bar{v}_z\end{bmatrix}^T \tag{11}$$

$$P_{est} = AP_{est}A^T + BQB^T + GLG^T \tag{12}$$

The same holds for the non-linear model, with the difference of having an EKF with linearised model matrices.
On top of what was already presented in subsection III-A, another feature that has to be taken into account is the possibility for the agent *i* to see *j* at a one-time step but not in the following. When this happens, *i* assumes that *j* is still using the input of the last communication and so uses it to propagate the dynamic, while it increases the uncertainty. This update continues until when *j* is seen again or the uncertainty on *j* grows above a pre-defined threshold. Note that this propagation requires that the applied inputs are exchanged during the data communication.

C. Local estimation of the global centroid

Each agent performs a local estimation of the global centroid by a weighted mean of the localisation of the others by the uncertainty on them. This implies that if a parachute does not know the position of any other (equivalent to knowing the location with high uncertainty), then it assumes that the centroid of the storm is itself. So, it applies the high-level control law only to itself.

D. Collision avoidance

Without losing generality, let us assume that the agent *i* performs the tessellation, while *j* is a different agent in the storm. Chute *i* has location $p_i = [x_i, y_i, z_i]^T$, a physical dimension inscribed in a circle of radius δ_i in the horizontal plane and $\delta_{z,i}$ in the vertical one, knows its position and the one of j with an uncertainty of respectively

$$diag(P_i^i) = \{{\sigma_{x,i}^i}^2, {\sigma_{y,i}^i}^2, {\sigma_{z,i}^i}^2\},\ diag(P_j^i) = \{{\sigma_{x,j}^i}^2, {\sigma_{y,j}^i}^2, {\sigma_{z,j}^i}^2\}$$

where P_i^i and P_j^i are the covariance matrices of the localization error of *i* and *j* respectively, and has a maximum linear velocity of $v_{max,i}$ $\left[\mathrm{m\,s^{-1}}\right]$ in the horizontal plane and $v_{max,zi}$ $\left[\mathrm{m\,s^{-1}}\right]$ in the vertical (such that the maximum displacement in one-time step is $s_i = v_{max,i}dt$ [m] and $s_{z,i} = v_{max,zi}dt$ [m] respectively).

1) Uncertainty in the localisation: The uncertainty in the self-localisation is taken into account by increasing the dimension of the agent δ_i as:

$$\tilde{\delta_i} = \delta_i + \kappa \max\left\{\sigma_{x,i}^i, \sigma_{y,i}^i\right\} \tag{13}$$

where κ is a coverage factor.
The uncertainty on the position of *j* is considered by projecting its location as:

$$\tilde{p_j} = p_j + \min\left\{\|p_i - p_j\|, \kappa \max\left\{\sigma_{x,j}^i, \sigma_{y,j}^i\right\}\right\} \frac{p_i - p_j}{\|p_i - p_j\|} \tag{14}$$

The min function is necessary to avoid the new agent *j* position falling behind the agent *i* itself.

2) Finite dimension and discrete-time dynamic: The finite dimension is taken into the picture by redefining the Voronoi area as follows:

$$\tilde{\mathcal{V}_i} = \begin{cases} \{q \in \mathcal{Q} | \|q - p_i\| \leq \|q - \tilde{p_j}\|\} & \Delta_i \leq \frac{\|p_i - \tilde{p_j}\|}{2} \\ \{q \in \mathcal{Q} | \|q - p_i\| \leq \|q - \hat{p_j}\|\} & \text{otherwise} \end{cases} \tag{15}$$

where $\Delta_i = s_i + \delta_i$ and

$$\hat{p_j} = \tilde{p_j} + \min\{2\delta_i, \|p_i - \tilde{p_j}\|\} \frac{p_i - \tilde{p_j}}{\|p_i - \tilde{p_j}\|} \tag{16}$$

Moreover, in the case when the centroid can reach the cell limit in one time step, the sensing range R_s has to be reduced, implying that the maximum Voronoi cell is shrunk at least of the dimension of the chute:

$$\tilde{R_s} = \begin{cases} R_s & \text{if } s_i + \delta_i > R_s \\ \max\{0, R_s - \tilde{\delta_i}\} & \text{otherwise} \end{cases} \tag{17}$$

Note that this approach requires only the knowledge of the dimension of the chute performing the tessellation.

3) Decentralisation of the algorithm: In the decentralised implementation of the algorithm, it is possible that the chute is not aware of the location of all the others in the storm, so it has to care only about the parachutes in a region of space around it. This subset of agents is called *neighbour set*, and it is defined as:

$$\mathcal{N}_i = \left\{\hat{p_j} \in \mathbb{R}^2 | \|p_i - \hat{p_j}\| < \tilde{R_{c,ij}}\right\} \tag{18}$$

with $\tilde{R_{c,ij}} = R_c + \kappa\left(\max\left\{\sigma_{x,i}^i, \sigma_{y,i}^i\right\} + \max\left\{\sigma_{x,j}^i, \sigma_{y,j}^i\right\}\right)$ to take into account also the uncertainties in the localisation. With this consideration in mind, the agent's cell is given by:

$$\hat{\mathcal{V}_i} = \left\{\tilde{\mathcal{V}_i} \cap \bar{\mathcal{C}}_{i,\tilde{R_s}}\right\} \tag{19}$$

where $\bar{\mathcal{C}}_{i,\tilde{R_s}}$ is the closure of the circle with radius $\tilde{R_s}$.

4) Extension to the 3D case: It is assumed that the agent performing the tessellation can detect the presence of the others even when they are above and below it in a range defined by R_{cv} (sensing range in the vertical direction). In particular, when another agent is detected within this range, it is included in the neighbour set as:

$$\tilde{\mathcal{N}_i} = \{p_j \in \mathcal{N}_i | |\Delta_z| < R_{cv} + \kappa\sigma_z^i + \frac{\Delta_z}{\|\Delta_z\|}\Delta s_z\} \tag{20}$$

where $\Delta_z = z_i - z_j$ is the height difference, $\Delta s_z = s_{z,i} - s_{z,j}$ is the difference between the maximum vertical displacements, and $\sigma_z^i = \sigma_{z,i}^i + \sigma_{z,j}^i$.
Since the parachute models have only a unidirectional actuation in the vertical direction (i.e., they can only brake their fall and not go upwards), the only limit necessary to identify the z-axis tessellation is the lower. This can be done by:

$$\mathcal{Z}_i = \begin{cases} \{q \in \mathcal{Q} | 0 \leq z_i - z_q \leq \Delta z - \delta_z - \kappa\sigma_z^i\} & \Delta_z \geq 0 \wedge i \in \tilde{\mathcal{N}_i} \\ \left\{q \in \mathcal{Q} | 0 \leq z_i - z_q \leq R_{sv} + \kappa\sigma_{z,i}^i\right\} & otherwise \end{cases} \tag{21}$$

where z_q is the generic point along the z-axis.

E. High-level motion control

1) Weights for the LQR: The only parameters to be set in the LQR control are the weight matrices S and R. By increasing the state matrix, the algorithm reduces the error between the actual state and the desired one, while increasing the input matrix minimises the input. They are usually competing objectives. Since the parachute inputs will be saturated

in the low-level control, there is no interest in using a big input matrix. At the same time, it is essential to have a good performance of the states to reduce the final distance between the global centroid and the target.

2) Same control for all the chutes: This is a simple control low because the agent applies the same input computed for the fake parachute representing the global centroid.

3) Inverse kinematics: Regarding the inverse kinematics, the postural task asks to make the single agents converge towards the global centroid to reduce the root mean square of the agents' distance from the global centroid and, eventually, from the target, thanks to the main task. The importance of this choice is explained further in the Results section. When using the postural task, the weighting value is set such that the closer the global centroid is to the target, the more importance is given to letting the single parachute converge toward the global centroid, with exponential behaviour. The pseudo-code of the inverse kinematics algorithm is presented in the Algorithm 1.

Algorithm 1 Numerical IK

- Find centroid error position e_c
- Find parachute error position e_x
- Find total error position $e = [e_c; e_x]$
- Find jacobian matrix J
- Initialize line search factor $\alpha = 1$
- Initialize weighting factor w

while $|e_c|^2 \geq 0.5$ & $|e_x|^2 \geq 0.1$
$\Delta x = (J^T J + w^2 I)^{-1}(J^T e_c + w^2 e_x)$
$x_{test} = x + \alpha \Delta x$
$x = x_{test}$
$e = e'$
end while

4) Managing of emergency case: As said before, the low-level control is performed after dividing the plane where the parachute moves with a Voronoi tessellation, considering all the agents in a surrounding space of the considered one. Even though it is, in principle, permissible for two agents having the same position in the xy plane and different heights, there are some situations in which this can create problems. For example, when an agent sees many others around it, its Voronoi cell may be reduced to a point because of having considered uncertainties and finite dimensions. If, in this case, it localises other agents below it with an xy location reasonably close to its own, then it will not be able to move to avoid the collision. To solve this issue, the *emergency control* tries to move the falling agent as far as possible from the new see ones. This is done by not considering the uncertainties in the tessellation (i.e. enlarging the Voronoi cell as much as possible) and moving in the opposite directions with respect to the sum of the vectors connecting itself and the considered ones.

F. Low-level motion control

While the algorithm calculates the value of the LQR gain, the values of the proportional gains of the low-level control have to be chosen. For the linear model gain of the equation (7), it is important to choose a value such that there is no risk of overshooting the target. This condition is avoided if the inequality (22) holds: in one step, the displacement given by the controller must not be greater than the target distance.

$$k_p \left(p_i - C_{\mathcal{V}_i}\right) dt \leq \left(p_i - C_{\mathcal{V}_i}\right) \Rightarrow k_p \leq 1/dt \qquad (22)$$

Regarding the non-linear model, on the other hand, the gain for the forward velocity is set to one, and the gain for the angular velocity is set such that in one time step, it is less than the maximum one (23) allowed by (10).

$$k_\omega = \omega_{max}/\pi \qquad (23)$$

Once the input is calculated and the error is summed to them to account for their errors, they are saturated to consider the actual performances. Even though the real actuator has not been identified, the errors' standard deviation of the actuators is set as 10% of the maximum permissible input, with a coverage factor of 3 (i.e. 99.73% of probability).

G. Conclusion of the simulation

When an agent touches the ground, it cannot move any more, and its control input is set to zero. However, the GPS signal continues to arrive, and the parachute continues communicating with the other agents and sending its position.

V. Results

A. Test of the Voronoi tessellation

Even though the Voronoi tessellation is performed in the 3D space, an example of implementation for two agents in the 2D plane is here presented in Figure 2 because it is more understandable. The communication ranges are $R_{c1} = 2.2, R_{c2} = 0.55$ and a coverage factor of $\kappa = 3$ has been used. Here three different cases are reported: A) agents with point dimensions and $s_{max} = 0$ (i.e. analogous to the continuous time implementation of the algorithm) and perfect localizations, B) finite physical encumbrance $\delta_1 = 0.25$, $\delta_2 = 0.15$, finite space $s_{max,1} = 1$, $s_{max,2} = 0.35$ and perfect localization, C) finite physical encumbrance, finite velocity and uncertainty in localization $\sigma_1^1 = \sigma_2^2 = 0.05^2 I_3, \sigma_1^2 = 0.1^2 I_3, \sigma_2^1 = 0 I_3$. In case A, agent *1* sees *2* inside its communication range and sets its cell limit at half their distance; chute *2* does not see *1* and so its cell becomes the whole circle with radius R_{c2}. In case B, agents *1* and *2* in one-time step can reach the limit of the cell, so they have to shrink their old cells of δ_1 and δ_2. The Voronoi limit of agent *2* moves inside the encumbrance of the chute itself. In case C, on top of what already happened in case B, *1* further shrinks its limits so that in the direction between *1* and *2* the limit goes above *1*. Meanwhile, *2* increases its encumbrance, reducing its Voronoi limit more than the dimension of the previous area, leading the final cell to be a point. In that final condition, *1* cannot move towards while *2*, while *2* cannot move at all.

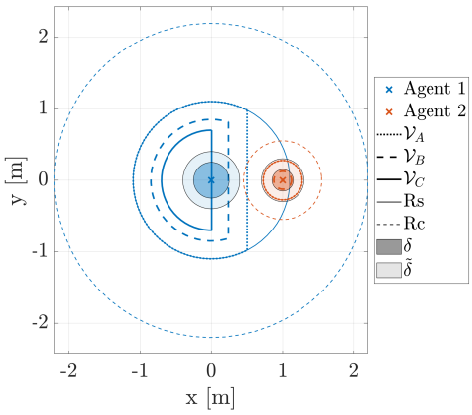

Fig. 2: Example of the Voronoi tessellation for two agents in the plane. $\mathcal{V}_A$ is build considering only the position of the agents, $\mathcal{V}_B$ considers finite dimensions and velocities while $\mathcal{V}_C$ considers also the uncertainties.

B. Example of localization

Figure 3 reports an example of the localization done by one agent on itself when the EKF uses the GPS measurement and the model (labelled *measure*) or only the latter (labelled *model*). In this specific example, nine agents fall from $[500, 500, 1000]$ toward $[0, 0, 0]$, with the inverse kinematic enabled and the probability of having the GPS measure equal to 50%. The iterations when the initial free-falling period and the landing on the ground are highlighted with dashed lines. It

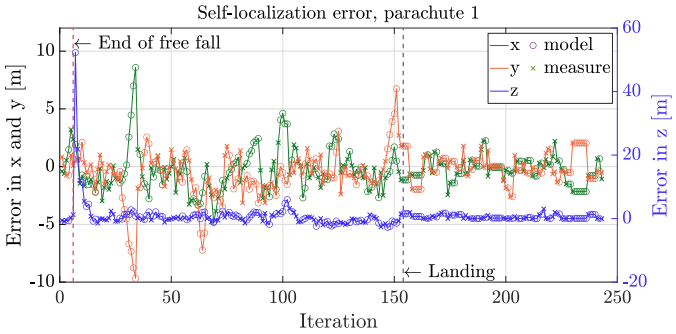

Fig. 3: Error in the self-localization done by agent 1, with a probability of having the GPS measure of 50%.

could be seen that after the end of the free-falling part when the parachute opens and the falling velocity suddenly reduces, the localization error grows a lot, while it quickly decreases in a few iterations. It is also interesting to notice how there are no GPS measurements between iterations 27 and 34, so the error made by localizing with only the model grows. At iteration 35, a new GPS signal is available, and the error is reduced. Finally, the errors are lower after the landing because wind and input noises no longer affect the agent's position.

C. Example of a complete swarm trajectory

Figure 4 shows the trajectory followed by 13 parachutes falling between the previous positions, while Figure 5 shows the time evolution of states and control inputs for one of the falling parachutes. The wind noise has been set to 3 $\left[\mathrm{m\,s^{-1}}\right]$ in every direction. It could be seen that the centroid (red

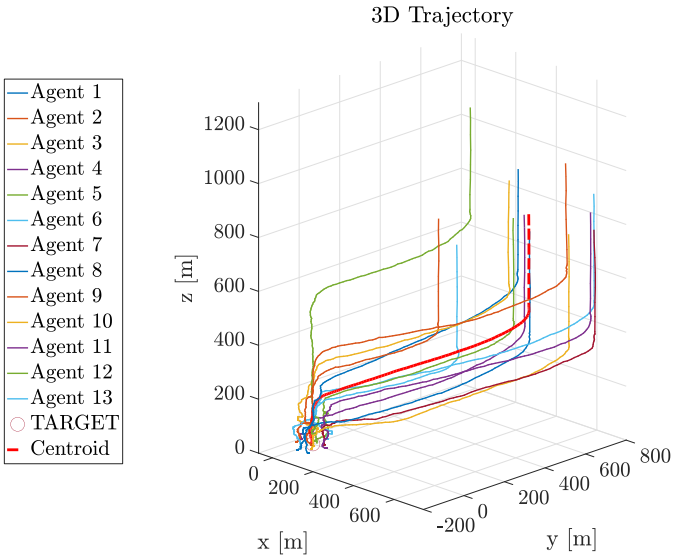

Fig. 4: 3D trajectory with 13 parachutes and all probabilities set to 1.

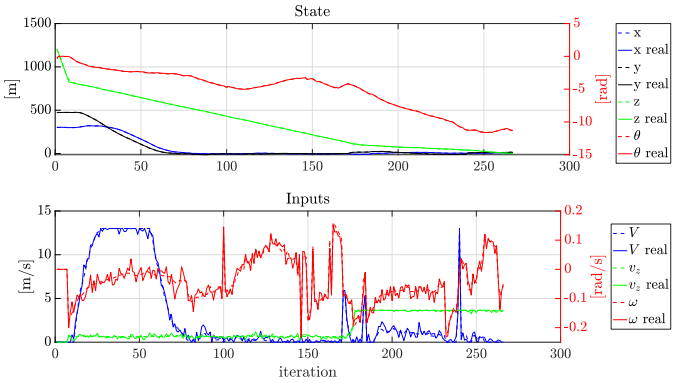

Fig. 5: States and inputs behaviour of agent 12.

dashed line of Figure 4) reaches the target correctly, while the parachutes fall around it without any collision.
Regarding the inputs, it may be noticed that there is no actuation in the initial free-falling part. In contrast, in the final part, the control on the z-axis is saturated to reduce the speed before contact with the ground. Also, the forward velocity is saturated in the central part, where the agent moves toward the target.

D. Distributed WLS

Figure 6 represents the standard deviation of the localization error committed by agent 7 of the simulation in V-B in the localization of the others before and after distributing information via the WLS algorithm in the three directions. It must be noted that *before WLS* considers the localization at the time steps when the relative distance measurement is

performed or when the dynamic of the other is propagated through the model. On the other hand, *after WLS* considers the result of the consensus algorithm, so in that instant, the localization can also be based only on the information shared by the network with the considered one. Note that, as expected

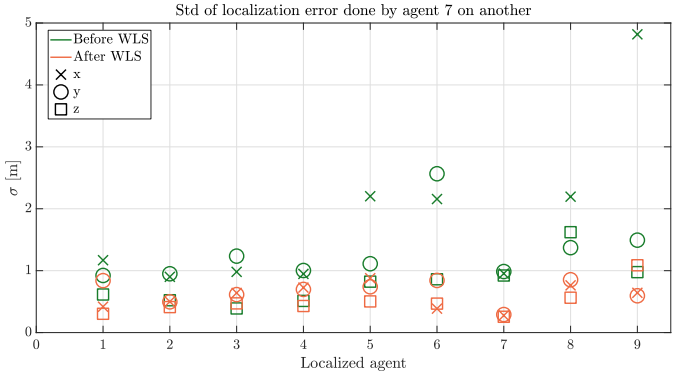

Fig. 6: Standard deviation of the error made by the parachute seven on the localization of the others.

after the WLS, the error in the localization is reduced for all the agents.

E. Effect of the Inverse Kinematics

A comparative test has been done to test the IK's effectiveness in the navigation. In particular, several parachutes have been driven with and without using the IK. The initial conditions of the two cases are the same for a given round, and more rounds have been run. No uncertainties and noises have been introduced to highlight the effect of the navigation only. Finally, the distance between the centroid and the target has been computed alongside the agent's Root Mean Square (RMS) to the target distance. The mean results among multiple rounds are collected in Table I. It could be seen that the IK approach reduces the dispersion of the chutes around the target, thanks to the postural task, for both models. In contrast, the distance of the global centroid from the target seems independent of the choice, except in the case of only one parachute. However, since having all the parachutes as near as possible to the target may be preferable, the RMS highlights the task's success.

TABLE I: Comparison between the use of IK or not

#	Linear				Non-linear			
	Dist.		RMS		Dist.		RMS	
	IK	No IK	IK	No IK	IK	No IK	IK	No IK
1	2.99	0.01	2.99	0.01	3.00	0.02	3.00	0.02
3	6.21	3.05	25.36	33.34	7.72	4.42	25.36	27.74
5	4.32	6.13	29.41	38.76	6.86	5.61	32.84	39.83
7	3.07	4.86	35.20	41.88	6.30	4.57	32.62	47.31
9	5.12	5.47	37.56	49.35	7.21	8.64	41.49	48.43
11	2.31	2.53	43.18	53.43	8.83	5.90	43.44	55.80
13	4.70	3.47	46.37	58.23	3.42	7.52	46.91	57.78

F. Effect of the probabilities

A parametric study has been conducted changing the probability of having the GPS or relative measurements between chutes, which simulates the ability of the real devices to acquire the data. This simulation considers nine parachutes of the nonlinear type affected by noise. The initial free-falling part and the final deceleration are turned off in the simulation because the localization takes some iterations to recover the error induced by the sudden change of vertical dynamics. In each test, one of the probabilities has been changed while the other has been kept constant at 100%. After the simulation, the standard deviation of the localization error in the three directions has been computed for the self-localization in Figure 7 and on the others in Figure 8. For the latter case, the mean of the error on all the others is reported. The graph shows that the GPS probability highly

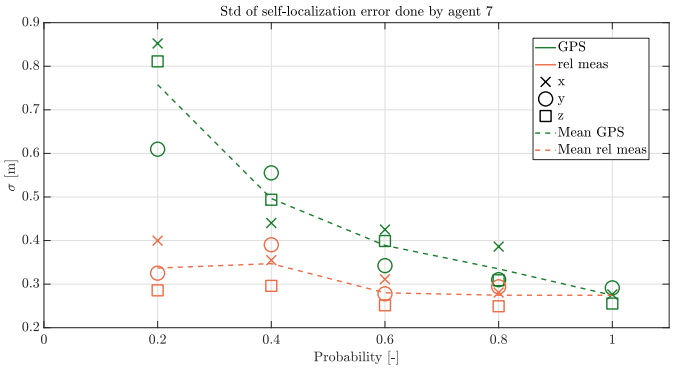

Fig. 7: Standard deviation of the localization error made by the parachute seven on itself at different values of GPS and relative measurements probabilities.

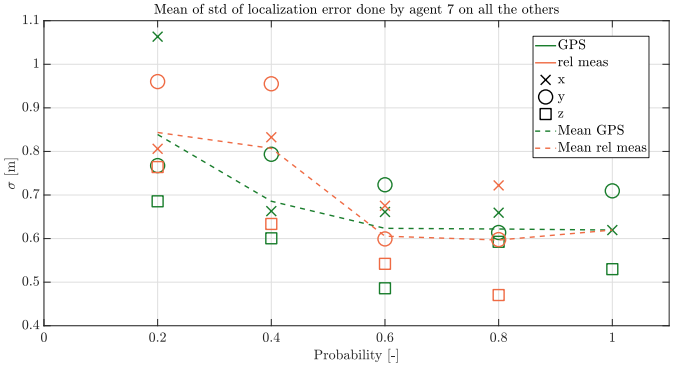

Fig. 8: Standard deviation of the localization error made by parachute seven on the other parachutes at different values of GPS and relative measurements probabilities.

affects the self-localisation error, while it is less by the relative measurement. This may be due to two facts. The first is that the GPS alone can provide good localization, so the further information added by the relative measurement has a small contribution to the estimation. Furthermore, the probability of having the relative measurement is conditioned by the distance between agents, which in our simulation depends on its evolution.

On the other hand, the two effects are more combined in the localization errors made on the others since, for this analysis, the

possibility of exchanging messages rules the process. In fact, when the agents are not close enough, they cannot exchange information with one another. Hence, the collected information (independently from its source) cannot be shared, and no contribution can be provided to the localization. Furthermore, when the connectivity is not always ensured, the effect of the error committed by propagating the states with the model is more significant.

VI. Conclusion

The project objectives have been successfully fulfilled since the parachute storm's centroid has been correctly driven from the initial point to the ground target. The prescribed centroid trajectory has been computed with an optimal controller, while two ways to coordinate the agents' movement have been proposed. The employed parachutes were a simple linear model and a more complicated unicycle-like nonlinear one, so two different control laws have been studied for them. Finally, no collisions between agents have been reported thanks to employing a control law based on the Voronoi tessellation.
Some aspects that can be included in the feature are:

- The presence of a minimum forward speed at which the parachute has always to fly;
- Consider the forces applied by real actuators instead of their overall effects on the velocities
- The possibility of unidirectional communications, leading to non-symmetric adjacency matrix;
- Implementation of a fully 3D Voronoi cell able to manage all the cases of inclusion of agents in all directions;
- Not discharging the self-localization information reached after the WLS round before using it in the new KF/EKF, this may be done with some more advanced localization algorithm, such as the Cooperative localization as described in [15].

References

[1] Martino, J., & Setters, D. (2020, July 27). Precision Motors help guided parachutes deliver cargo. Tech Briefs. https://www.techbriefs.com/component/content/article/tb/supplements/mct/features/applications/11837

[2] Precision guided parachutes - maxongroup.us. Available at: https://www.maxongroup.us/medias/sys_master/root/8803679404062/Precision-Guided-Parachutes.pdf?attachment=true (Accessed: 01 July 2023).

[3] Ultra-Wideband RTLS, Positioning, & Sensor Technology Available at: https://www.inpixon.com/technology/standards/ultra-wideband#:~:text=What%20is%20the%20Range%20of,sight%20between%20devices%20or%20anchors. (Accessed: 07 September 2023).

[4] La velocità di un paracadutista con un paracadute aperto. Velocità di caduta del paracadutista. (no date) Kemtalant. Available at: https://kem-talant.ru/it/bodybuilding/skorost-parashyutista-s-raskrytym-parashyutom-skorost.html (Accessed: 21 August 2023).

[5] La dimensione del paracadute. (no date) Kemtalant. Available at: https://www.sportsrec.com/7305468/the-size-of-skydiving-parachutes (Accessed: 21 August 2023).

[6] Britannica, The Editors of Encyclopaedia. "parachute". Encyclopedia Britannica, 7 Aug. 2023, https://www.britannica.com/technology/parachute. Accessed 21 August 2023.

[7] F.A.Q. — Skydive Lucca (no date) Scuola di paracadutismo Lucca. Available at: http://www.paracadutismolucca.it/f-a-q/ (Accessed: 21 August 2023).

[8] Kim, Y., & Bang, H. (2019). Introduction to Kalman Filter and Its Applications. IntechOpen. doi: 10.5772/intechopen.80600

[9] Manuel Boldrer, Luigi Palopoli, Daniele Fontanelli, A unified Lloyd-based framework for multi-agent collective behaviours, Robotics and Autonomous Systems, Volume 156, 2022, 104207

[10] S. Ahmad and M. O. Tokhi, "Linear Quadratic Regulator (LQR) approach for lifting and stabilizing of two-wheeled wheelchair," 2011 4th International Conference on Mechatronics (ICOM), Kuala Lumpur, Malaysia, 2011, pp. 1-6, doi: 10.1109/ICOM.2011.5937119.

[11] Benhabib, B. & Goldenberg, Andrew A. & Fenton, R.. (2007). A Solution to the Inverse Kinematics of Redundant Manipulators. Journal of Robotic Systems. 2. 373 - 385. 10.1002/rob.4620020404.

[12] Aristidou, A. & Lasenby, J. Inverse kinematics: a review of existing techniques and introduction of a new fast iterative solver. (University of Cambridge, Department of Engineering,2009)

[13] İşleyen, A., Wouw, N. & Arslan, Ö. Feedback Motion Prediction for Safe Unicycle Robot Navigation. (2023)

[14] Daniele Fontanelli, Notes of the course "Intelligent distributed systems", 2022/2023

[15] S. S. Kia, S. Rounds and S. Martinez, "Cooperative Localization for Mobile Agents: A Recursive Decentralized Algorithm Based on Kalman-Filter Decoupling," in IEEE Control Systems Magazine, vol. 36, no. 2, pp. 86-101, April 2016, doi: 10.1109/MCS.2015.2512033.

This report is the final document for the "Distributed Systems for Measurement and Automation" course.